Composites Part B 178 (2019) 107457

Contents lists available at ScienceDirect

Composites Part B

journal homepage: www.elsevier.com/locate/compositesb

Synergetic effects of carbon nanotubes and triblock copolymer on the lap shear strength of epoxy adhesive joints

Jojibabu Panta[a], Y.X. Zhang[a,b,*], Andrew N. Rider[c], John Wang[c], Gangadhara Prusty B.[d]

[a] School of Engineering and Information Technology, The University of New South Wales, Canberra, ACT, 2600, Australia
[b] School of Computing, Engineering and Mathematics, Western Sydney University, Sydney, NSW, 2751, Australia
[c] Aerospace Division, Defence Science and Technology Group, Melbourne, Victoria, 3207, Australia
[d] ARC Training Centre for Automated Manufacture of Advanced Composites (AMAC), School of Mechanical and Manufacturing Engineering, UNSW Sydney, NSW, 2052, Australia

ARTICLE INFO

Keywords:
Adhesive bonding
Lap shear strength
Epoxy
Triblock copolymers
Carbon nanotubes
Functionalization

ABSTRACT

This paper investigated the effect of functionalized CNTs and triblock copolymer addition on the lap shear strength of the epoxy adhesive joints. CNTs were functionalized using an ultrasonicated-ozonolysis process to enhance the uniform and stable dispersion of CNT, and 3-roll mill was employed to achieve the uniform distribution of CNT in the epoxy matrix. Two different triblock copolymers named as SBM and MAM were used as toughening agents to improve the shear strength of the nanocomposite adhesive material. Single lap shear tests were performed on the aluminum adhesively bonded joints using pure and modified epoxy adhesives to determine the shear strength of the adhesive. The effect of different weight fractions of untreated CNTs, functionalized CNTs, and the hybrid effect of CNTs and triblock copolymer addition on the shear strength of the adhesive joints was studied. It was found that the use of functionalization and 3-roll mill methods are effective to achieve stable and even dispersion of the CNTs and the shear strength was improved by 26% (23.6 MPa) compared to that of pure epoxy. The hybrid effect of functionalized CNTs and SBM showed the maximum shear strength of 44.7 MPa, with an increase of 137% compared to that the of the pure epoxy demonstrating the effectiveness of the triblock copolymer addition in improving the shear strength. Fracture analysis revealed that the nano-additives acted synergistically to increase fracture ductility which contributed to increase the shear strength. In addition, glass transition temperature and thermal stability of the modified epoxy were found to be relatively unaffected.

1. Introduction

The use of epoxy adhesives has become extensive in recent years due to their exceptional ability to join dissimilar and complex parts in aerospace and automobile industries comparing to conventional joining methods such as fasteners, riveting and welding. Epoxy adhesive joints offer excellent adhesion properties, uniform stress distribution, good corrosion resistance and high strength to weight ratio [1,2]. Despite these advantages, unmodified epoxy resins used as adhesives inherently have low fracture toughness due to high cross-linking density, which limits their general usage in structural applications [3,4].

Recent developments in nanotechnology show that the addition of nanostructured materials may improve the mechanical properties of epoxy nanocomposites in terms of stiffness and toughness [5–7]. It is well known that the incorporation of carbon nanotubes (CNTs) in epoxy resins offers an opportunity to develop new composite materials with superior mechanical properties. The high Young's modulus and tensile strength of the CNTs relative to that of epoxy adhesives make them good candidates for reinforcement [8,9]. A number of studies on CNT/epoxy composites adhesives materials have been conducted and achieved the highest lap shear strength improvement of about 40–50% by incorporating 0.5–3 wt% of CNTs [10–12]. For example, Srivastava [13] has obtained a 41% increase in the lap shear strength with 3 wt% of CNT reinforcement over the pure epoxy joints. Jojibabu et al. [14] reported that the incorporation of 1 wt % of CNT into epoxy led to 53% enhancement in the joint strength.

However, the uniform and stable dispersion of CNTs in an epoxy matrix have been a notorious and critical issue, which restricts the performance of the nanocomposites [15,16], as well as the strength of the adhesive joints [13,14]. Besides, the interfacial adhesion between

* Corresponding author. School of Computing, Engineering and Mathematics, Western Sydney University, Sydney, NSW, 2751, Australia.
E-mail address: sarah.zhang@westernsydney.edu.au (Y.X. Zhang).

https://doi.org/10.1016/j.compositesb.2019.107457
Received 19 June 2019; Received in revised form 9 September 2019; Accepted 15 September 2019
Available online 18 September 2019

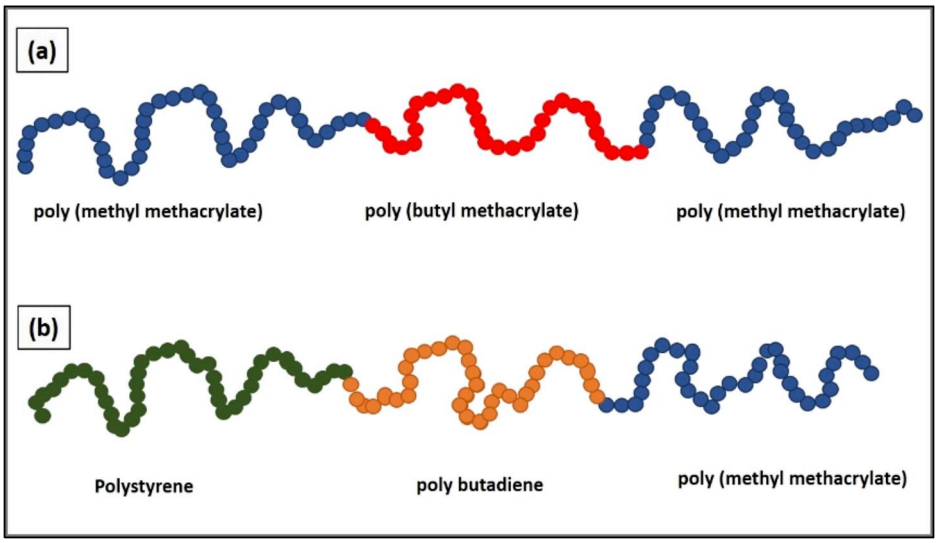

Fig. 1. Molecular structure of BCPs a) MAM symmetric copolymer with a centre block of poly (butyl methacrylate) surrounded by poly (methyl methacrylate) b) SBM copolymer comprised of three different blocks, Polystyrene, polybutadiene and poly (Methyl methacrylate).

the CNTs and the epoxy matrix is another important issue, which also influences the performance of the CNT/epoxy adhesives. It is well known that the functionalization of CNTs is a foremost technique to increase their degree of dispersion and enhance the interfacial adhesion with the polymeric matrices [8]. A significant research effort has been devoted to study the chemistry of CNT functionalization [17–19] process that can improve the interfacial interactions with the epoxy matrix and reduce the formation of CNT agglomerates. The commonly used functionalization methods to modify the CNT surface include strong acids [20–22], surfactants [23,24] and coupling agents [25,26]. Sydlik et al. [27] have studied the effect of different chemical functionalization methods on the joint strength of the CNT/epoxy composite adhesive joints. They found that the joint strength was increased by 36% and 27% for the optimized functionalized CNTs compared to that of the pure epoxy and untreated-CNT/epoxy respectively.

Although the chemical functionalization methods have been proven to be effective, they still have some discrepancies in practical applications. The use of strong acids, whilst introducing functional groups and eliminating impurities, could cause structural damage to CNTs. The use of surfactants is a less aggressive method for creating stable dispersions but is difficult to remove from the treated CNTs. Furthermore, the use of harmful acids and solvents are not environment-friendly, and they must be recycled after the treatment.

Recently, an environmentally friendly method called ultrasonicated ozonolysis (USO) was used for functionalizing carbon nanomaterials [28,29]. The functionalization of CNTs using ozone treatment is relatively high efficient and economical when compared with the other commonly used methods [30]. The USO process produces stable and aqueous dispersions which are free of harsh chemicals. The simultaneous circulation of ozone progressively oxidizes the CNTs, while ultrasonication breaks down the CNT agglomerates. During ozone treatment, ozone reacts with unsaturated carbon double bonds of carbon surfaces through the Criegee mechanism [31]. Chiang et al. [32] demonstrated that the ozonation of CNTs could increase the oxygen functional groups and the specific surface area, which in turn improved the adsorption capacity of the activated carbon. The previous literature [33,34] reported that the ozone treatment of CNTs could enhance the level of dispersion of CNTs and promote good interfacial bonding with the epoxy matrix. Najafi et al. [35] observed that the ozone treatment of CNTs increased the solubility in N,N-dimethylformamide by 320% compared to that of untreated CNTs. Tang et al. [34] studied the interface quality between the ozone-treated CNTs and epoxy matrix using Raman spectroscopy as a function of temperature ranging from −60 °C to 60 °C. Their results showed that the ozone-treated CNTs have stronger interfacial bonding with the epoxy matrix compared with the untreated CNTs. It was also reported that the stress transfer between the ozone-treated CNT and epoxy interface is higher than the untreated-CNT/epoxy interface.

On the other hand, a lot of research efforts have been made to increase the fracture toughness of epoxy matrix which is a typical demerit of the material. Extensive research has been conducted on the effect of various block copolymers (BCPs) on the fracture toughness of the bulk epoxy resins [36,37]. BCPs are exceptional materials, which have been used to increase the toughness of the epoxy by the formation of unique nanostructures within the epoxy matrix with less impact on stiffness and glass transition temperature (T_g). BCPs can self-assemble into disordered spherical micelles, vesicles or cylindrical (wormlike) micelles in the epoxy matrix [37]. These final structures influence the mechanical performance of the original epoxy resins. BCPs such as poly (methyl methacrylate)-poly (butyl methacrylate)-poly (methyl methacrylate) (MAM), and poly (styrene)-poly (butadiene)-poly (methylmethacrylate) (SBM), which can be synthesized on an industrial scale, have shown significant increase in the fracture toughness of the epoxy resins [36,38,39].

Quite a notable amount of reports could be found dealing with the influence of BCPs and their nanostructures on the mechanical performance of the bulk epoxy systems [36,39–42]. However, the adhesion properties of the BCP/epoxy composites as adhesive materials are still poorly covered in the literature in spite of the increasing attention in adhesives and sealants manufacturing industries [43]. In addition, no data regarding the hybrid effect of CNTs and BCP incorporation on the adhesion performance of the epoxy resins have been reported.

The aim of this work is to carry out a systematic study of the effect of CNTs and BCP additions on the lap shear strength of the epoxy adhesive joints, which could be useful for the development of high-performance structural epoxy adhesive materials. CNTs were functionalized using USO process to enhance the uniform and stable dispersion and interfacial interactions in the epoxy matrix. CNTs were dispersed in the epoxy matrix using 3-roll mill up to 10 passes to achieve the uniform distribution in the matrix. The homogeneity of CNTs dispersion and the effectiveness of USO treatment were analyzed using optical microscopy, field emission gun scanning electron microscope (FEGSEM) and Raman spectroscopy. On the other hand, two different BCPs, such as SBM and MAM were used as toughening agents to increase the shear strength.

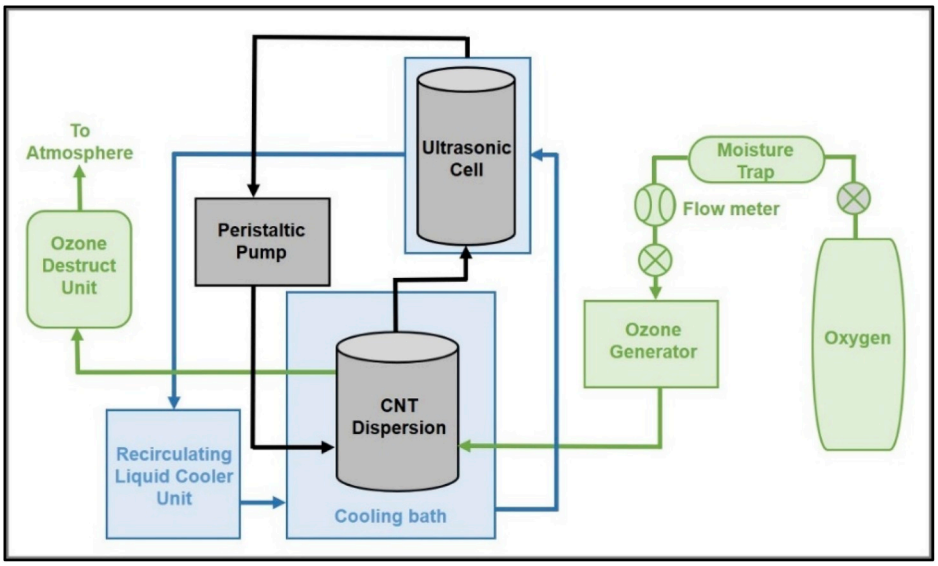

Fig. 2. Schematic representation of USO treatment of carbon nanotubes [19].

ATR-FTIR was performed to study the molecular interactions between the CNTs, BCP and the epoxy matrix of the modified composites. The effect of various amounts of untreated CNTs, USO treated CNTs, BCP addition and the hybrid effect of functionalized CNTs and BCP on the shear strength of the adhesive joints is studied. To understand the structure property-relation and mechanism of the increase in lap shear strength, the fracture surfaces of the adhesive joints were investigated using FEGSEM. Differential scanning electron calorimetry (DSC) and thermogravimetric analysis (TGA) studies were also carried out to observe the effect of the addition of CNTs and BCP on the thermal stability of the nano-modified epoxy adhesives.

2. Materials and sample preparation

2.1. Materials

Diglycidyl ether of bisphenol-A (DGEBA) epoxy resin K3600 purchased from Huntsman, Australia was used as the matrix. Multi-walled CNTs of diameter 10–15 nm and length 10–20 μm (Hanwha Chemicals, Republic of Korea) and two types of BCPs namely, MAM M51 and SBM E21 (Arkema, France) were used as epoxy resin modifiers. The schematic representation of MAM and SBM is shown in Fig. 1. When the BCP mixed with an epoxy resin, both the polybutadiene (PB), Polystyrene poly (butyl methacrylate) (PBuA) blocks yields a soft immiscible rubber phase, whilst the poly (methyl methacrylate) block ensure compatibility with the epoxy.

2.2. Functionalization of CNTs

The USO treatment was applied to CNTs with the aim of producing oxygen functional groups on the CNT sidewalls which react with the epoxy chains and provides good interfacial adhesion. The USO treatment is the simultaneous process of ultrasonication and the ozonisation. The role of ozone treatment is to oxidize the CNTs and introduce the hydroxyl and carboxyl groups on the CNTs while the ultrasonication process deagglomerates the CNT aggregates. Fig. 2 shows the schematic representation of the functionalization of CNTs using USO treatment. Moisture-free oxygen with a flow rate of 500 mL/min passed through an ozone generator and treated the CNTs at 5 °C while the aqueous-CNT mixture is continuously circulated by a peristaltic pump through a mixing cell 16 h. The full details of functionalization of carbon nanomaterials using USO process can be found in previously reported work by our co-workers [28].

2.3. Dispersion of BCPs in the epoxy adhesive

The BCP was first dried at 110 °C for 3 h and then ground using a laboratory mortar and pestle. Then the BCP was dispersed and dissolved within the epoxy resin with a loading of 10 wt%. Epoxy resin was stirred at 80 °C for 30 min and the fine BCP was gradually added to epoxy resin.

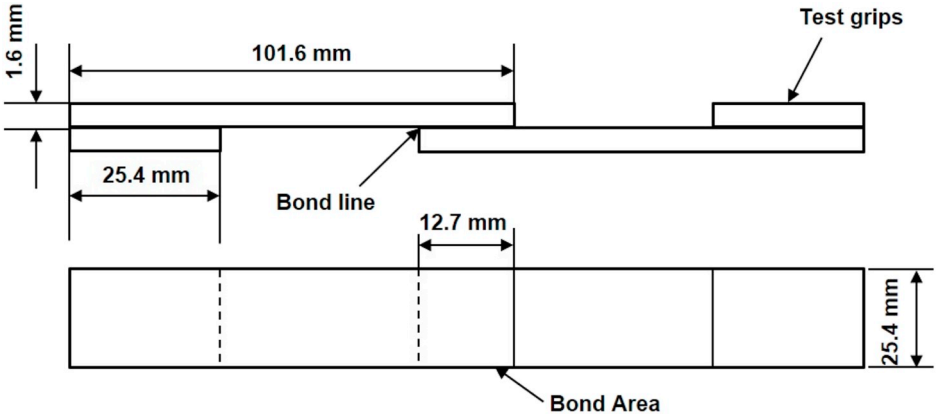

Fig. 3. Single lap shear joint as per the ASTM D1002.

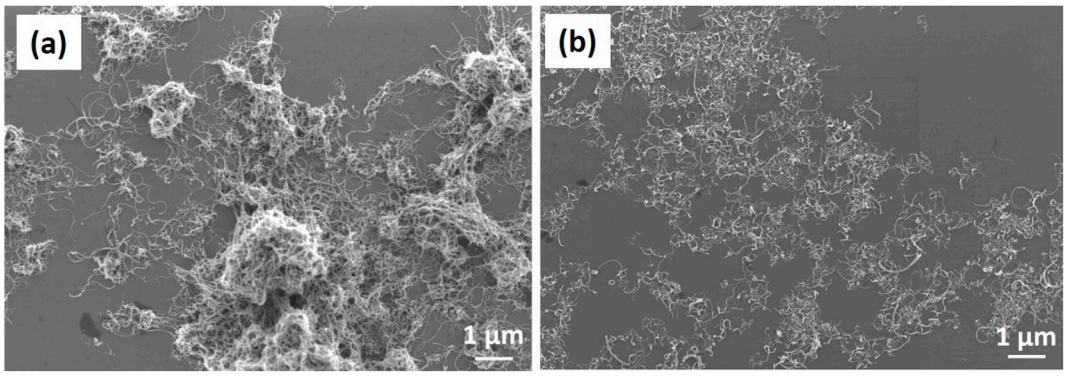

Fig. 4. FEGSEM images of a) untreated and (b) OZ-CNTs treated for 16 h by USO.

The BCP/epoxy mixture was stirred at 80 °C until complete dissolution was observed (usually within 12 h). The hardener was then added to the mixture (100:30 by weight) and mixed using a planetary centrifugal mixer (THINKY, Japan) for 10 min at 1,000 rpm followed by vacuum degassing at room temperature for 30–45 min. The final mixture was used as the adhesive to prepare the lap shear joints for the shear test to determine the lap shear strength.

2.4. Dispersion of CNTs in the epoxy adhesive

The epoxy resin and CNTs were taken in required amounts to prepare 0.2, 0.5, 0.7, 1.0 and 2.0 wt% CNT/epoxy mixture. Initially, the epoxy resin and CNTs were pre-mixed using a planetary mixer at 1,000 rpm for 15 min. The CNT/epoxy mixture was then mixed using a three roll-mill (EXACT 80E, Germany) at 180 rpm. The gap size between the 1st and the 2nd roller was 20 µm, the 2nd and the 3rd roller was 5 µm. It was found that the CNTs were dispersed homogeneously in the epoxy matrix after 10 passes. The hardener was then added to the CNT/epoxy mixture and mixed for 10 min using planetary mixer at 1,000 rpm followed by vacuum degassing at room temperature for 30–45 min to entrap the air bubbles formed during mixing process.

2.5. Preparation of lap shear joints

Single lap shear test on adhesive joints is often used to examine the bond strength. The single lap shear joints were prepared as per the ASTM D1002 standard (Fig. 3). Aluminium alloy 2024-T3 sheets with 1.6 mm thickness (Aerospace materials, Australia) were used as adherends for preparing lap shear joints. The dimensions of aluminium 2024-T3 substrates were 101.6 mm × 25.4 mm × 1.6 mm and bonding area was 25.4 mm × 12.7 mm. The previous literature [44,45] showed that the maximum lap shear strengths were obtained for the joints with the adhesive thickness of up to 0.1–0.2 mm. Therefore, the thickness of the adhesive layer was maintained at 0.15 mm by shim placement.

Prior to joint preparation, the surface of the aluminium adherends was surface treated to achieve the maximum joint performance. The aluminium adherends were first cleaned with Methyl Ethyl Ketone (MEK) solvent (Bio strategy, Australia), to remove the grease at the surface and the release agents followed by abrasion (Scotch-Brite 3 M No. 447, 3 M, Australia) and cleaning with clean-room wipes (Boeing distribution services, Australia) soaked in MEK. This process was then repeated using deionised water. The adherends were then grit blasted using aluminium oxide grit (AccuBRADE-50, Coltronics, Australia) with a grit size of 50 µm at 450 kPa pressure to obtain a rough surface. The grit blasted samples were then immersed in a solution consisting of 1% γ-glycidoxypropyltrimethoxysilane (Sigma Aldrich, Australia) and 99% distilled water for 60 min at room temperature. The presence of γ-glycidoxy propyltrimethoxysilane in the aqueous solution promotes chemical bond with the fresh and active aluminium oxide layer. At the other side, the silane has a reactive epoxy group that is reactive to the epoxy adhesive. The aluminium substrates were then dried at 110 °C for 1 h followed by cooling to room temperature [46].

3. Experimental programs

3.1. Raman spectroscopy

Raman spectra of the untreated and USO treated CNTs (OZ-CNTs) were recorded using a Hyperion 1000 mid-infrared microscope attached to Raman spectrometer (Bruker Vertex 70, Germany) with a 20X magnification objective lens using a microscope and a 532 nm laser. The spectra of the samples were obtained between 3,500 and 500 cm^{-1} at a resolution of 2 cm^{-1} with a laser energy of 5 mW to ensure that no sample degradation occurred during collection. The spectra were collected by accumulating 10 scans and using an exposure time of 2 s for each scan to achieve a reasonable signal-to-noise ratio.

3.2. Microstructural characterization

The state of agglomeration of CNTs before and after USO treatment was observed using a field emission gun scanning electron microscope (FEGSEM) (ZEISS Merlin, Germany) operating at 5 kV. The untreated and ozone-treated CNTs were diluted in deionised water to 0.1 g/L and deposited onto a silicon wafer followed by ambient drying. Optical microscopy images were then captured at 100X magnification on a small droplet of the uncured CNT/epoxy mixture placed on a microscope glass to examine the level of dispersion after each stage of mixing. Dispersion at the sub-micron scale was examined on fracture surfaces of the adhesive joints using FEGSEM with a carbon coating (~3 nm thick) to provide a conductive film to prevent charging during imaging.

3.3. Fourier transform infrared spectroscopy (FTIR)

Attenuated total reflectance (ATR)-FTIR (Bruker Vertex 70, Germany) studies were performed on the pure epoxy and CNT and BCP mixtures between 4000 and 600 cm^{-1} at a resolution of 4 cm^{-1}. Spectra were normalised to the maximum intensity peak at 2920 cm^{-1} to enable qualitative comparison in chemistry for the different mixtures.

3.4. Thermal characterization

The glass transition temperature (T_g) of epoxy adhesives with CNTs and BCPs was measured using differential scanning calorimetry (NETZSCH 204 F1 Phoenix, Germany) under argon atmosphere at a flow rate of 65 ml/min with 5 mg samples in aluminium pans using a constant heating rate of 10 K/min from −50 °C temperature to 150 °C.

The thermal stability of the epoxy and nanocomposites was studied using a thermogravimetric analyzer (NETZSCH STA 449C Jupiter,

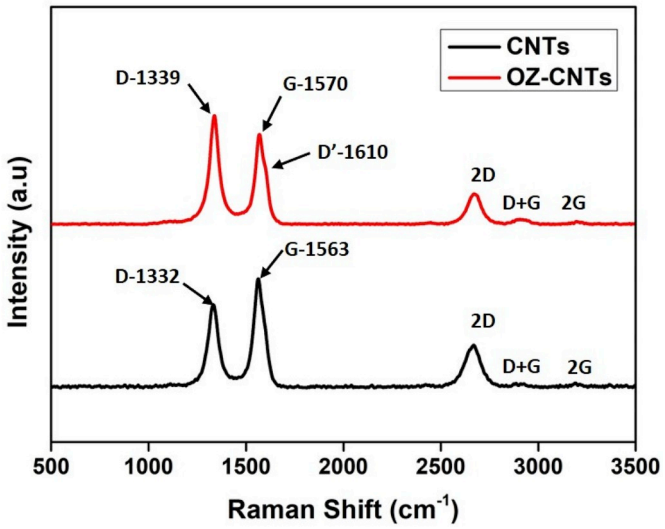

Fig. 5. Raman spectra of untreated and USO treated CNTs.

Germany) by heating cured samples to 600 °C with a ramp rate of 10 K/min under argon atmosphere.

3.5. Mechanical testing of adhesive joints

Single lap shear tests were conducted on the adhesive joints using a universal tensile testing machine (MTS 100 kN, USA). The adhesive joints were subjected to tensile loading with a strain rate of 1.3 mm/min as per the ASTM D1002 standard. For measuring the shear strength of the adhesive joints, five samples were tested for each material.

4. Results and discussions

4.1. CNT functionalization

The FEGSEM images shown in Fig. 4 compare the OZ-CNTs with untreated CNTs. It was found that the untreated CNTs were highly entangled due to the van der Waals attraction forces, while the OZ-CNTs were much more evenly dispersed across the surface. This shows that the USO treatment has facilitated a reduction in agglomerates but has also led to a shortening of the CNT length due to scission caused by the high-powered ultrasonic horn used in the reactor.

Raman spectra of untreated CNTs and OZ-CNTs are shown in Fig. 5. The intensity of the D band at 1332 cm^{-1} shows the presence of defects in the untreated CNTs prior to USO treatment. After USO treatment there is an increase in the D band intensity and the G band has shifted from 1563 cm^{-1} to 1568 cm^{-1}, with a second component becoming noticeable at 1610 cm^{-1}. This corresponds to an increase in the oxidation level of the CNTs with USO treatment and a corresponding increase in structural disorder, suggesting some ozone reaction is occurring away from pre-existing defect sites. There is also an obvious decrease in intensity of the 2D band at 2698 cm^{-1} and a small increase in the D + G band at 2941 cm^{-1} for OZ-CNTs, also consistent with an increased level of oxidation in the CNTs. The intensity ratio of the D to G bands, I_D/I_G, was measured at 0.76 with untreated CNTs and increased to 1.21 after 16 h of ozone treatment.

4.2. CNT dispersion in the epoxy

The optical microscopy images of the 0.5 wt% CNT/epoxy mixtures at different levels of mixing are shown in Fig. 6. It was observed that the CNT/epoxy dispersions after pre-mixing by planetary mixer showed loosely packed aggregates of CNTs formed due to van der Waals attraction forces. The 3-roll mill was used to mix the CNT into the epoxy and after 10 passes an even dispersion was achieved. The aggregate sizes decreased after each pass of three-roll milling. In the final mixing stage

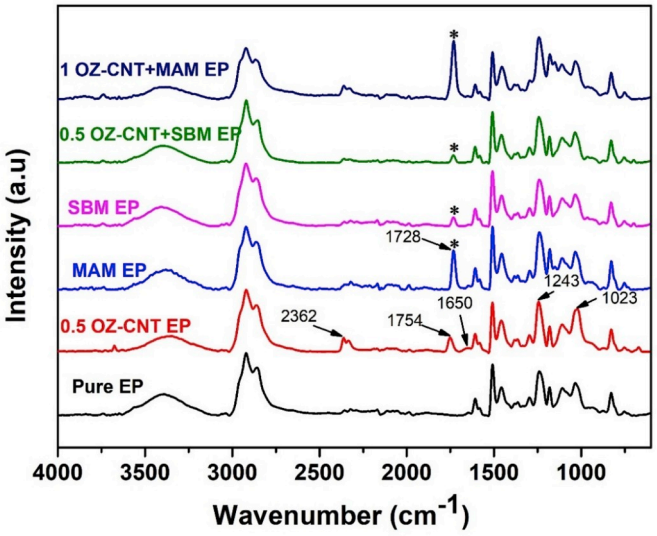

Fig. 7. Comparison of ATR-FTIR spectra of epoxy composites with OZ-CNTs and BCPs.

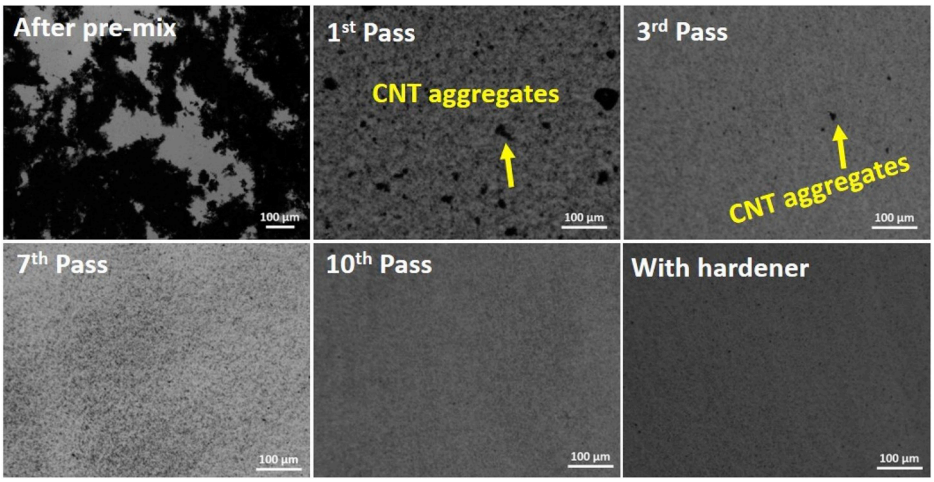

Fig. 6. Optical micrographs of 0.5 wt% CNT/EP mixture after pre-mix (planetary mixing) and three-roll milling at different passes.

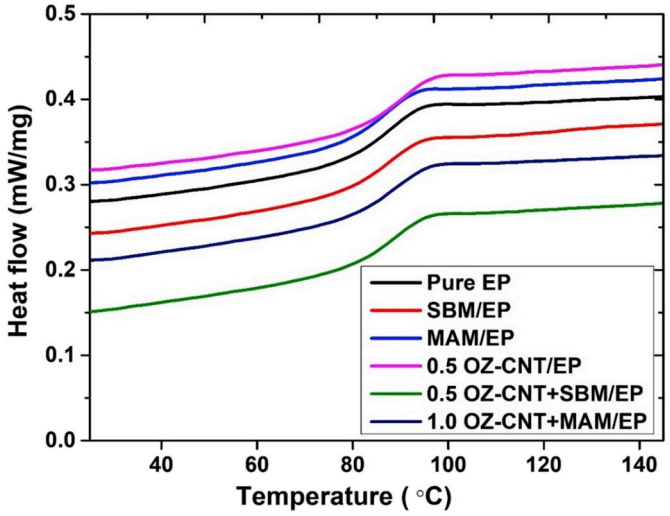

Fig. 8. DSC thermograms for cured pure epoxy and optimized composite adhesives.

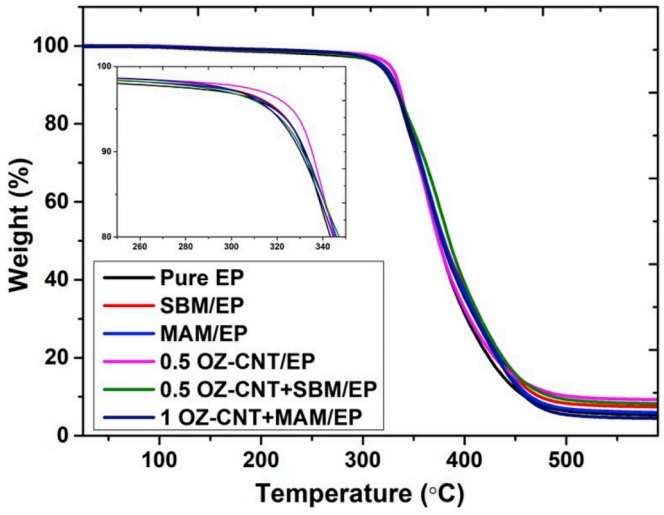

Fig. 9. TGA curves of cured pure epoxy and optimized composite adhesives.

Table 1
Glass transition and onset degradation temperatures of pure and modified epoxy adhesives.

Sample name	Glass transition temperature T_g (°C)	Onset degradation temperature (°C)
Pure EP	87.6 ± 0.2[a]	326.6
SBM/EP	88.2 ± 0.5[a]	325.9
MAM/EP	86.9	323.5
0.5 OZ-CNT/EP	90.5	328.0
0.5 OZ-CNT + SBM/EP	89.1	328.3
1.0 OZ-CNT + MAM/EP	88.2	325.2

[a] Indicates average of two samples, the other values correspond to one tested sample.

with hardener, the CNTs were homogeneously dispersed in the epoxy.

ATR-FTIR was performed to study the molecular interactions between OZ-CNTs, BCP and epoxy after mixing and cure of thin-film samples. Fig. 7 shows absorbance spectra of pure epoxy and composite adhesives between 4000 and 600 cm^{-1}. In pure epoxy adhesive, the bands at 3440, 1023 and 1245 and 915 cm^{-1} correspond to O–H stretching, stretching of C–O–C ether, aliphatic ether C–O–C and stretching C–O of the epoxy group, respectively. A possible reaction mechanism would involve epoxide ring rupture due to reaction with the carboxyl (-COOH) groups on the CNTs [47]. It was reported that the ozone treatment produces two distinct surface-bound functional groups, such as esters (corresponding to 1754 cm^{-1}) and quinones (corresponding to 1650 cm^{-1}) as well as gas-phase CO_2 (corresponding to 2362 cm^{-1}) [48]. Hong et al. [47] reported that the formation of new band 1754 cm^{-1} is the evidence of good adhesion of –COOH groups on the OZ-CNTs with the epoxy matrix by esterification. The formation of a new peak corresponding to 1754 cm^{-1} in the OZ-CNT/EP composite implies that OZ-CNTs have reacted with the epoxy matrix. A new ester peak was also observed at 1728 cm^{-1} for the BCPs modified epoxy. The alteration of C═O and OH absorption groups may have resulted from the hydrogen bonding between carbonyl groups of PMMA in BCPs and hydroxyl epoxy [49,50]. Hence, this specific interaction with epoxy is believed to have influenced the nanostructure development in the BCP modified epoxy adhesives. It was also observed that the intensity of the 1726 cm^{-1} peak is higher for MAM/EP, which would be consistent with a higher content of PMMA in the MAM BCP compared to the SBM BCP. The peak intensity at 1726 cm^{-1} is more pronounced after adding OZ-CNTs to the BCP modified epoxy adhesives. Therefore, the FTIR results suggest that OZ-CNTs and BCPs have chemically interacted with epoxy in the nanocomposite adhesives.

4.3. Thermal characterisations

Thermal characterization studies were performed to observe the effect of incorporation of CNTs and BCPs on the thermal stability of the composites. The DSC thermograms of the pure epoxy and modified epoxy adhesive are shown in Fig. 8 and the values are depicted in Table 1. Hydro and Pearson [36] indicated that the decrease in T_g of the BCP/epoxy composites represented the incomplete phase separation of BCP in the epoxy matrix. In the current study, both SBM and MAM appeared to be more completely miscible and phase-separated as there was no significant decrease in the T_g. On the other hand, the T_g of 0.5 wt % OZ-CNT/EP showed minimal change compared to the pure epoxy, which is due to the CNTs in the epoxy matrix restricting the epoxy chain mobility, resulting in greater thermal stability [51]. Allaoui et al. [52] reviewed the effect of single-walled CNTs in epoxy nanocomposites on the T_g and reported a decrease of 6–24 °C, possibly caused by the bundling tendency of CNTs. On the other hand, 1 wt % of multi-walled CNTs showed up to 3 °C increase in T_g of the epoxy nanocomposites. From the current study, we observed that the T_g increased by about 3 °C, at a relatively low 0.5 wt% of OZ-CNTs, suggesting good CNT dispersion within the epoxy relative to previous studies. For hybrid nanocomposites, slight increases in T_g values were observed, compared to that of pure epoxy and BCP modified epoxy.

Fig. 9 shows the effect of OZ-CNTs and BCP dispersion on the thermal decomposition temperature of the epoxy adhesives. The onset degradation temperatures (at which decomposition starts) of pure and modified epoxies are given in Table 1. The TGA results revealed that there was no deterioration in thermal stability for the BCP modified epoxy adhesives. In addition, the OZ-CNT/EP showed a slight increase due to the OZ-CNTs, suggesting that the OZ-CNTs could act as gas barriers to retard the permeation of volatile gasses during thermal exposure.

4.4. Lap shear strength of the adhesive joints

The effect of incorporation of the two BCPs and different weight fractions of CNTs on the lap shear strength of epoxy adhesive joints is shown in Fig. 10. As the weight fraction of CNTs in the epoxy increases, the joint strength reaches a maximum value of 22.1 MPa at 0.5 wt% (Fig. 10a). Previous work has attributed the enhanced lap shear strength of the adhesive joints to an increase in stiffness and strength provided by

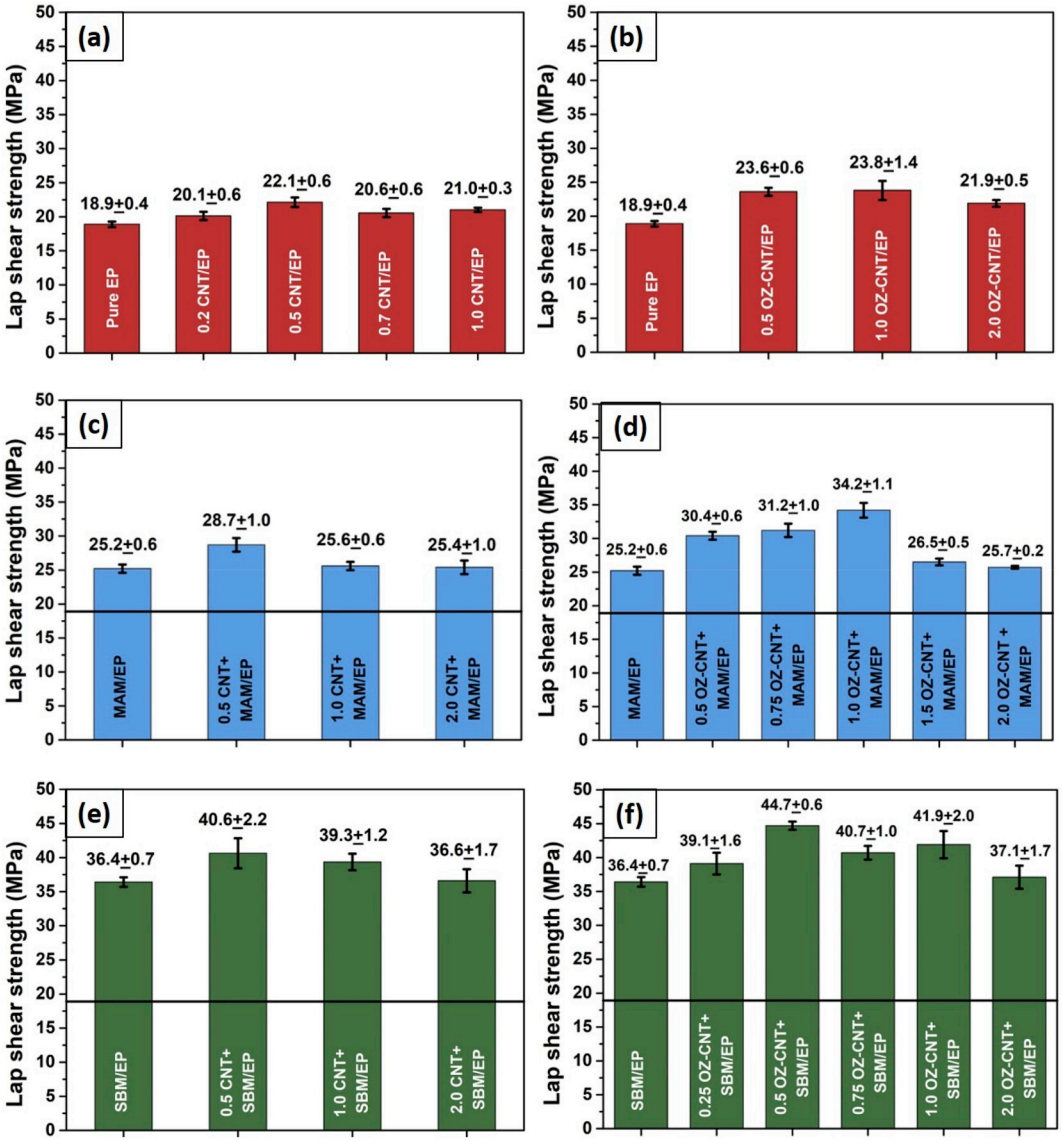

Fig. 10. Lap shear strength of the adhesive joints a) CNT/EP, b) OZ-CNT/EP, c) CNT + MAM/EP, d) OZ-CNT + MAM/EP, e) CNT + SBM/EP, and f) OZ-CNT + SBM/EP. The black line (in c-f) indicates the lap shear strength of the pure EP.

the CNT filler [13]. However, CNTs also provide enhanced toughness, which may also contribute to the observed increase [53], particularly, in the lap-shear configuration used in current testing, where adherend rotation during loading can lead to high peel stresses at the joint edges.

The OZ-CNT/EP joints, Fig. 10b showed further improvement in the lap shear strength as compared to the untreated CNT/EP joints in Fig. 10a. Significantly, the USO treatment leads to a higher strength at a higher weight fraction of CNTs, which indicates that the USO processing has helped improve the dispersion and reduced the size of the critical agglomerates that cause the observed reduction in lap shear strength above 0.5 wt% in the untreated CNT/EP joints. Even at 2 wt% OZ-CNT/EP, the lap shear strength is comparable to the highest strength measured for the untreated CNT/EP joint strength at 0.5 wt%, indicating the significant improvement the USO processing has provided in creating well-dispersed nanocomposite materials.

Fig. 10c ande shows that the addition of 10 wt% of the BCPs MAM and SBM, respectively, leads to a significant increase in the lap shear strength compared to the pure epoxy or the CNT/epoxy joints, particularly the SBM addition, providing a 93% increase over the pure epoxy. In contrast to SBM, the MAM addition resulted in only 33% increase in shear strength, indicating the sensitivity of the BCP chemistry and the relative effect of the different nanophase morphologies and the associated cavitation mechanisms that contribute to the increased epoxy toughening.

The lap shear strength was further increased with the addition of CNTs in the BCP modified epoxy. The maximum lap shear strength of 34.2 MPa was observed for the 1.0 wt% OZ-CNT + MAM/EP, while 44.7 MPa was achieved for the 0.5 wt% OZ-CNT + SBM/EP joints, which is 81% and 137% higher than that of the pure epoxy joints, respectively. The combination of SBM and OZ-CNT appears to produce an increase in strength which is greater than the improvements realised by the nano-additives used separately by around 10%, suggesting that the two materials interact favourably to enhance shear strength of the joint.

4.5. Fractography

In order to study the homogeneity of the CNTs dispersion and nanostructure formed by BCP in the epoxy, the fractured surfaces of the adhesive joints were investigated by FEGSEM. The FEGSEM micrographs of the fracture surfaces resulting from the pure epoxy and 0.5 wt % OZ-CNT/EP joints are shown in Fig. 11. The fracture surface of the pure epoxy (Fig. 11a) was typical of brittle, glassy fracture observed in

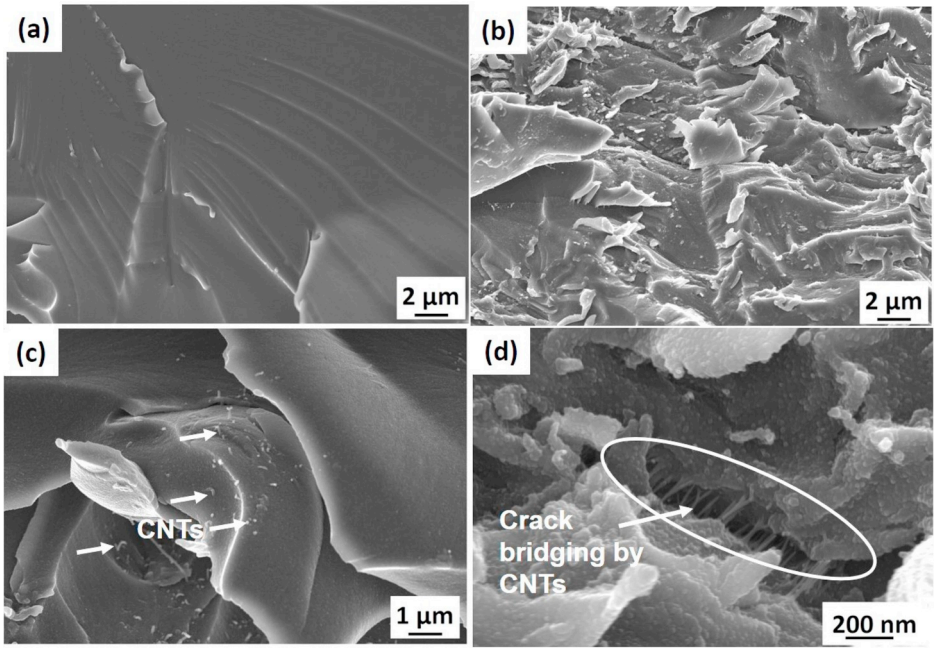

Fig. 11. FEGSEM images of the fracture surface of adhesive joints (a) Pure EP, (b) 0.5 wt% OZ-CNT/EP (c and d) high magnification images of 0.5 wt% OZ-CNT/EP.

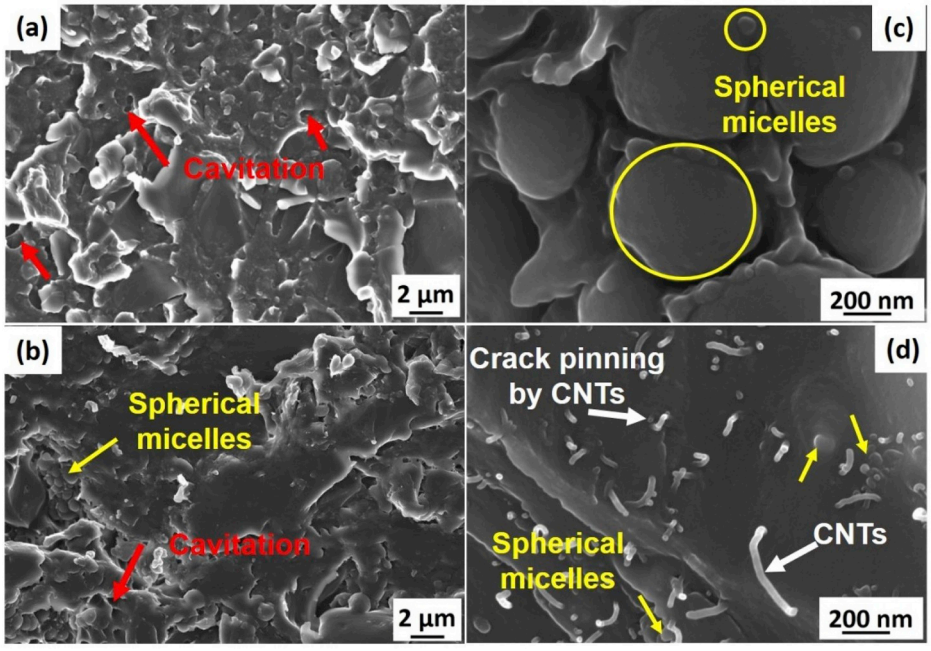

Fig. 12. FEGSEM images of the fracture surface of adhesive joints (a) MAM/EP, (b) 1 wt% OZ-CNT + MAM/EP, (c and d) high magnification images of MAM/EP and 1 wt% OZ-CNT + MAM/EP, respectively.

shear failure, with fracture lines revealing low resistance crack propagation paths. From the fracture surface of the OZ-CNT/EP (Fig. 11b and c), the OZ-CNTs appear to be distributed homogeneously in the epoxy matrix without large agglomerates and the fracture surfaces reveal a more ductile fracture morphology. There is also evidence that the CNTs have adhered to the epoxy matrix with limited evidence of pull-out and CNTs encapsulated with thin layers of epoxy on the fracture surfaces. In addition, it can be seen from the high magnification image (Fig. 11d) that crack propagation was restricted by CNT bridging. The improved adhesion between the OZ-CNT and epoxy would be expected to increase the resistance to pull-out and debonding at the crack-tip and may help increase the fracture toughness of the OZ-CNT/EP adhesive.

Fig. 12 shows the MAM modified epoxy with and without OZ-CNTs. The failure surface images of the MAM/EP showed more plastic deformation and a rougher morphology when compared to the pure epoxy (Fig. 12a). Furthermore, spherical micelles ranging from 10 to 500 nm were observed in the MAM/EP adhesives, as shown in Fig. 12c. The distribution of spherical MAM domains throughout the epoxy matrix allowed uniform plastic deformation and considerable shear yielding. Cavitation is one of the significant features for rubber toughened epoxy systems [42,54]. In the BCPs used in the current adhesives, the voids created by the cavitation of the soft thermoplastic phase of the BCP

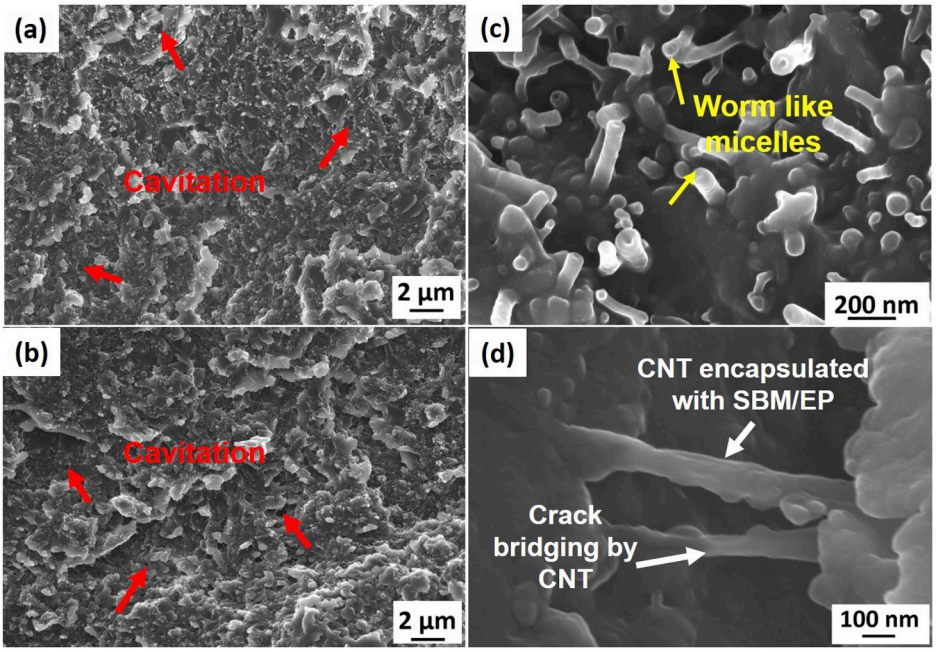

Fig. 13. FEGSEM images of the fracture surface of adhesive joints (a) SBM/EP, (b) 0.5 wt% OZ-CNT + SBM/EP, (c and d) high magnification images of SBM/EP and 0.5 wt% OZ-CNT + SBM/EP respectively.

restrict the crack propagation and facilitate plastic shear deformation of the epoxy matrix [42]. The cavities observed in the MAM/EP suggest that cavitation followed by plastic void growth could be one of the toughening mechanisms that contributed to the increased lap shear strength of the joints. In contrast, Fig. 12b shows the fracture surfaces of the 1 wt% OZ-CNT + MAM/EP joints where the fracture mechanism for the ternary composite adhesives involves plastic void growth post cavitation and CNT crack pinning (Fig. 12d) when the shear band

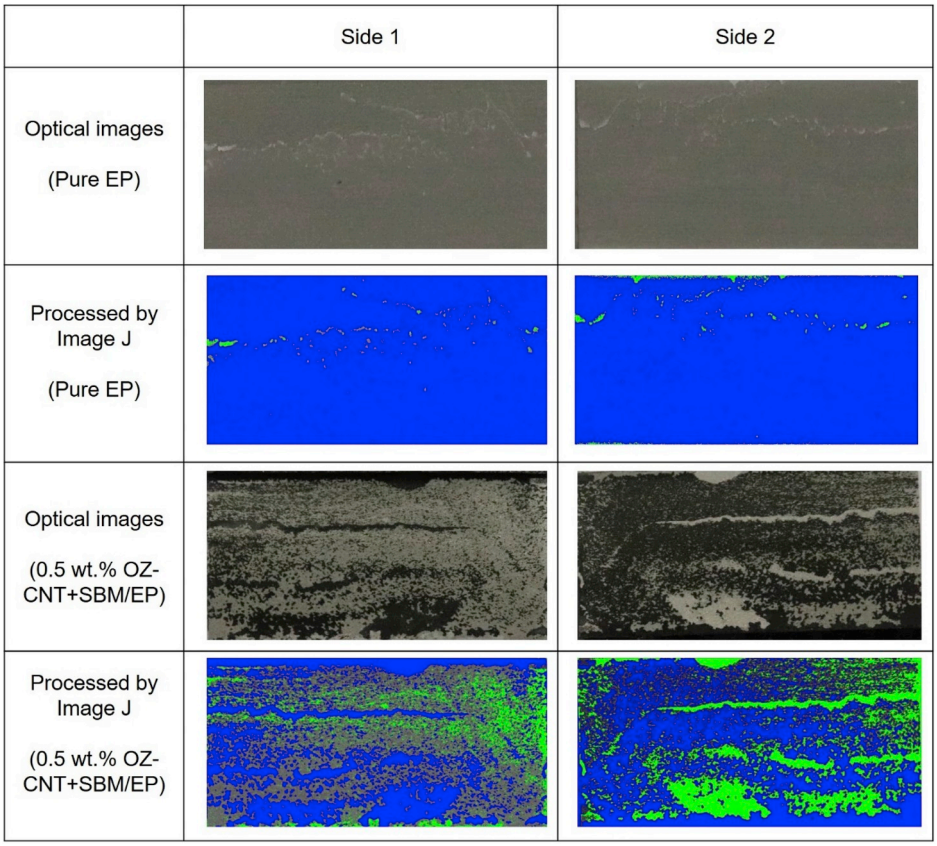

Fig. 14. Fracture surfaces of pure and 0.5 wt% OZ-CNT + SBM/EP lap shear joints, showing the relative percentages of cohesive failure with the adhesive (blue) and cohesive failure near the interface (green). (For interpretation of the references to colour in this figure legend, the reader is referred to the Web version of this article.)

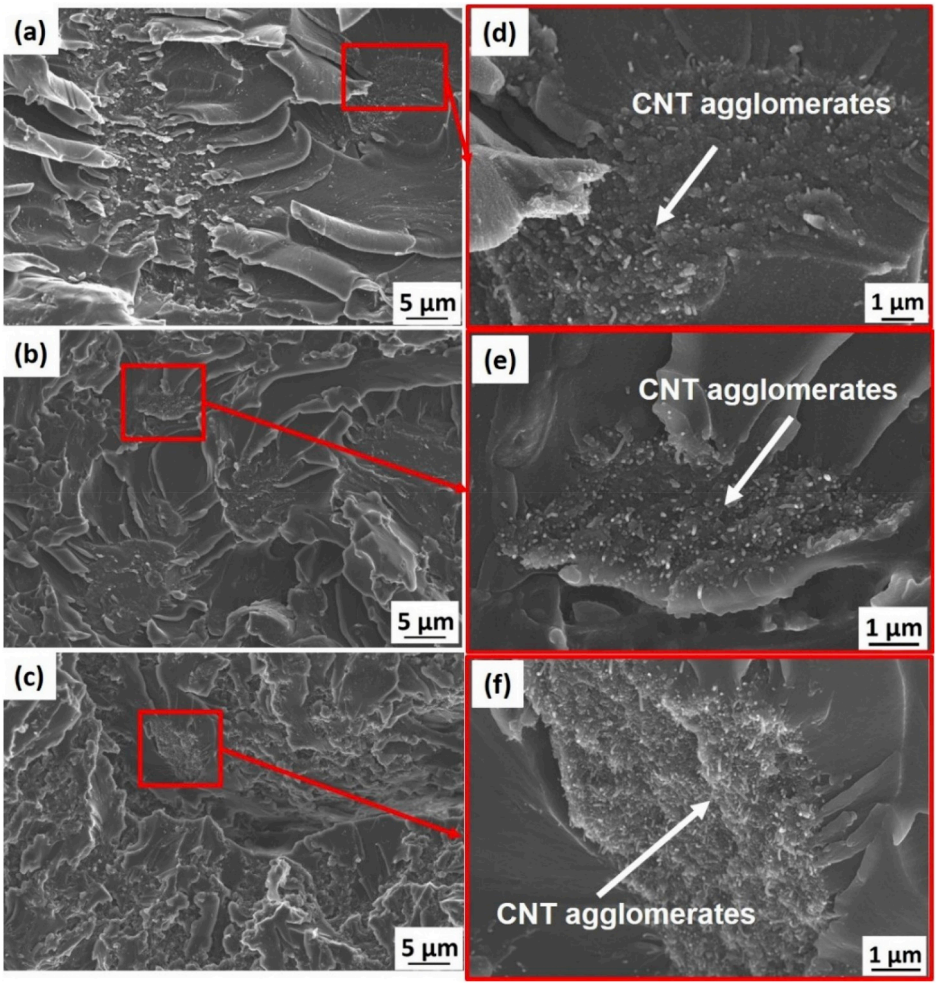

Fig. 15. FEGSEM images of fracture surface of adhesive joints (a) 2 wt% OZ-CNT/EP, (b) 2 wt% OZ-CNT + MAM/EP (c) 2 wt% OZ-CNT + SBM/EP, (d, e and f) high magnification images of 2 wt% OZ-CNT/EP, 2 wt% OZ-CNT + MAM/EP and 2 wt% OZ-CNT + SBM/EP respectively.

formation in the matrix proceeds. The presence of rigid CNTs may extend the level of cavitation and consequently the level of shear yielding that can occur in the epoxy matrix by increasing the critical crack length. The evidence of some CNT pull-out in Fig. 12d may suggest that the increased plastic yielding of the matrix, compared to the OZ-CNT/EP samples (Fig. 11c and d), places greater stress at the OZ-CNT/epoxy interface.

The fracture surfaces of the SBM modified epoxy in Fig. 13 show that the SBM particles were well dispersed in the epoxy. Fig. 13a also shows that the addition of SBM leads to surface morphology with a finer roughness texture when compared to the MAM/EP and pure epoxy joints, indicating even greater levels of plastic deformation. The SBM particles form a cylindrical or worm-like structure with a stiff PS core, which is covered with smaller PB fibrils, as shown in see Fig. 13c. Dean et al. [55] indicated that the strong interfacial bonding by the reactive functionalities resulted in the formation of such fibril structures. Liu et al. [56] stated that the spherical micelles exhibited reduced cavitation and matrix shear yielding upon fracture compared to the worm-like micelles. In addition, interfacial debonding or crack bridging is likely to be reduced because of the small size of the spherical micelle particles. Consequently, the MAM/EP adhesive exhibited a lower lap shear strength than the SBM/EP. Fig. 13d shows that the OZ-CNTs are encapsulated with SBM/EP, indicating good bonding with the matrix. It also suggests that the crack propagation is restricted by CNT bridging. The fracture mechanisms of the hybrid modified epoxies adhesives are believed to include the processes observed in the SBM/EP and the OZ-CNT/EP joints, which are the cavitation of the worm-like micelles, CNT bridging, and the improved plastic deformation in the epoxy matrix due to the localized plasticization of the SBM-EP interface. The absence of CNT pull-out in the SBM/CNT/EP samples (Fig. 13) also suggests that the increased plastic yielding accommodated by the SBM cavitation mechanism has reduced the interfacial stress at the CNT/epoxy interface when compared to the MAM/CNT/EP adhesive (Fig. 12d).

4.6. Failure modes of the adhesive joints

From the fracture surfaces of the pure and the composite adhesive joints, it was observed that all the joints failed cohesively. Optical images for complementary fracture surfaces of pure and 0.5 wt% OZ-CNT + SBM/EP adhesive joints are shown in Fig. 14. The failure surface texture was measured using ImageJ software [57]. It was found that the pure epoxy adhesive joints failed 100% cohesively within the adhesive layer, whereas, the 0.5 wt% OZ-CNT + SBM/EP joints showed a mixture of cohesive failure within the adhesive (93%) and cohesive failure in closer proximity to the adhesive and aluminium adherend interface (7%). The failure surfaces confirm that the surface treatment provided excellent adhesion, but the nanophase additions have moved the fracture plane closer to the adhesive-aluminium interphase region, which is commonly observed in higher strength structural adhesives [58].

FEGSEM analysis was also conducted on the 2 wt% OZ-CNT reinforced joints to identify the reasons for the reduction in strength observed for the optimal CNT loadings at 0.5 wt%. Fig. 15 shows the low

and high magnification fracture surface images. Large CNT agglomerates up to 10 μm in diameter can be observed for each of the samples. These CNT-rich agglomerates may be expected to act as localised stress concentrations within the adhesive and act as critical crack initiation sites that would reduce the ability of the bondline to achieve the same levels of shear yielding observed in the more homogeneous bondlines with lower CNT weight fractions [14].

Fig. S2 (in supplementary information) shows the Weibull distribution plot and the Weibull modulus for pure and modified epoxy adhesive joints at 0.5 wt% of OZ-CNTs. The Weibull modulus decreases with the addition of OZ-CNTs, and SBM relative to the pure epoxy samples but is clearly greater for the OZ-CNT and SBM used in combination. The increased Weibull modulus suggests that the OZ-CNT and SBM combine to reduce the sensitivity of the joint variation to material inhomogeneities or reduce the population of critical defects in the joint, consistent with the observed joint strength and fracture analysis mechanisms discussed.

5. Conclusions

The effect of incorporation of BCPs and different weight fractions of CNTs on the lap shear strength of the epoxy adhesive joints was investigated. Optical micrographs showed that the CNTs were well dispersed in the epoxy resin after 10 passes of three-roll milling. The maximum lap shear strength of 34.2 MPa was observed for 1.0 wt% OZ-CNT + MAM/EP, while 44.7 MPa was observed for 0.5 wt% OZ-CNT + SBM/EP joints, which was 81% and 137% higher than that of the pure epoxy joints, respectively. The components present in the BCPs were found to significantly alter the fracture mechanisms observed in the adhesive joints, with SBM worm-like micelles providing the most effective toughening enhancements. In contrast, the MAM spherical micelle particles showed reduced levels of cavitation and associated matrix shear yielding, resulting in the MAM/EP adhesives exhibiting lower lap shear strength than the SBM/EP. The present study shows that there is some synergistic improvement in the lap shear strength for the developed epoxy system, without reduction of the glass transition and thermal decomposition temperatures, often observed in traditional rubber toughened systems. The presence of BCPs act to induce shear yielding of the matrix by relieving the applied stress condition with mechanisms such as cavitation and/or debonding of the toughening phase. Simultaneously, the OZ-CNTs further increase the joint ductility by stiffening the matrix and extending the shear cavitation in the BCP phase, leading to enhanced shear yielding.

Acknowledgements

The grant support from the Department of Defence and the facility support from Defence Science and Technology Group, Melbourne. Support from Dr. Richard Muhrer and the Advanced Material Characterizations facility at Western Sydney University for microstructural characterizations are acknowledged.

Appendix A. Supplementary data

Supplementary data to this article can be found online at https://doi.org/10.1016/j.compositesb.2019.107457.

References

[1] Banea M, da Silva LF. Adhesively bonded joints in composite materials: an overview. Proc Inst Mech Eng L J Mater Des Appl 2009;223(1):1–18.
[2] Kumar A, Kumar K, Ghosh PK, Rathi A, Yadav KL. Raman, MWCNTs toward superior strength of epoxy adhesive joint on mild steel adherent. Compos B Eng 2018;143:207–16.
[3] Chang T, Brittain J. Studies of epoxy resin systems: Part D: fracture toughness of an epoxy resin: a study of the effect of crosslinking and sub-Tg aging. Polym Eng Sci 1982;22(18):1228–36.
[4] Jia Z, Feng X, Zou Y. An investigation on mode II fracture toughness enhancement of epoxy adhesive using graphene nanoplatelets. Compos B Eng 2018;155:452–6.
[5] Bhattacharya M. Polymer nanocomposites—a comparison between carbon nanotubes, graphene, and clay as nanofillers. Materials 2016;9(4):262.
[6] Wichmann MH, Schulte K, Wagner HD. On nanocomposite toughness. Compos Sci Technol 2008;68(1):329–31.
[7] Zakaria MR, Md Akil H, Abdul Kudus MH, Ullah F, Javed F, Nosbi N. Hybrid carbon fiber-carbon nanotubes reinforced polymer composites: a review. Compos B Eng 2019;176:107313.
[8] Ma P-C, Siddiqui NA, Marom G, Kim J-K. Dispersion and functionalization of carbon nanotubes for polymer-based nanocomposites: a review. Compos Appl Sci Manuf 2010;41(10):1345–67.
[9] Coleman JN, Khan U, Blau WJ, Gun'ko YK. Small but strong: a review of the mechanical properties of carbon nanotube–polymer composites. Carbon 2006;44(9):1624–52.
[10] De Cicco D, Asaee Z, Taheri F. Use of nanoparticles for enhancing the interlaminar properties of fiber-reinforced composites and adhesively bonded joints—a review. Nanomaterials 2017;7(11):360.
[11] Ahmadi Z. Nanostructured epoxy adhesives: a review. Prog Org Coat 2019;135:449–53.
[12] Nemati Giv A, Ayatollahi MR, Ghaffari SH, da Silva LF. Effect of reinforcements at different scales on mechanical properties of epoxy adhesives and adhesive joints: a review. J Adhes 2018;94(13):1082–121.
[13] Srivastava V. Effect of carbon nanotubes on the strength of adhesive lap joints of C/C and C/C–SiC ceramic fibre composites. Int J Adhesion Adhes 2011;31(6):486–9.
[14] Jojibabu P, Jagannatham M, Haridoss P, Ram GDJ, Deshpande AP, Bakshi SR. Effect of different carbon nano-fillers on rheological properties and lap shear strength of epoxy adhesive joints. Compos Appl Sci Manuf 2016;82:53–64.
[15] Coleman JN, Khan U, Gun'ko YK. Mechanical reinforcement of polymers using carbon nanotubes. Adv Mater 2006;18(6):689–706.
[16] Pandey G, Thostenson ET. Carbon nanotube-based multifunctional polymer nanocomposites. Polym Rev 2012;52(3):355–416.
[17] Tasis D, Tagmatarchis N, Bianco A, Prato M. Chemistry of carbon nanotubes. Chem Rev 2006;106(3):1105–36.
[18] Sun Y-P, Fu K, Lin Y, Huang W. Functionalized carbon nanotubes: properties and applications. Acc Chem Res 2002;35(12):1096–104.
[19] Balasubramanian K, Burghard M. Chemically functionalized carbon nanotubes. Small 2005;1(2):180–92.
[20] Park O-K, Chae H-S, Park GY, You N-H, Lee S, Bang YH, Hui D, Ku B-C, Lee JH. Effects of functional group of carbon nanotubes on mechanical properties of carbon fibers. Compos B Eng 2015;76:159–66.
[21] Kim JA, Seong DG, Kang TJ, Youn JR. Effects of surface modification on rheological and mechanical properties of CNT/epoxy composites. Carbon 2006;44(10):1898–905.
[22] Zhu J, Kim J, Peng H, Margrave JL, Khabashesku VN, Barrera EV. Improving the dispersion and integration of single-walled carbon nanotubes in epoxy composites through functionalization. Nano Lett 2003;3(8):1107–13.
[23] Vaisman L, Wagner HD, Marom G. The role of surfactants in dispersion of carbon nanotubes. Adv Colloid Interface Sci 2006;128–130:37–46.
[24] Geng Y, Liu MY, Li J, Shi XM, Kim JK. Effects of surfactant treatment on mechanical and electrical properties of CNT/epoxy nanocomposites. Compos Appl Sci Manuf 2008;39(12):1876–83.
[25] Kim MT, Rhee KY, Park SJ, Hui D. Effects of silane-modified carbon nanotubes on flexural and fracture behaviors of carbon nanotube-modified epoxy/basalt composites. Compos B Eng 2012;43(5):2298–302.
[26] Park S-H, Bandaru PR. Improved mechanical properties of carbon nanotube/polymer composites through the use of carboxyl-epoxide functional group linkages. Polymer 2010;51(22):5071–7.
[27] Sydlik SA, Lee J-H, Walish JJ, Thomas EL, Swager TM. Epoxy functionalized multi-walled carbon nanotubes for improved adhesives. Carbon 2013;59:109–20.
[28] Yeo ES, Mathys GI, Brack N, Thostenson ET, Rider AN. Functionalization and dispersion of carbon nanomaterials using an environmentally friendly ultrasonicated ozonolysis process. JoVE (Journal of Visualized Experiments) 2017;(123):e55614.
[29] Rider A, An Q, Thostenson E, Brack N. Ultrasonicated-ozone modification of exfoliated graphite for stable aqueous graphitic nanoplatelet dispersions. Nanotechnology 2014;25(49):495607.
[30] Li M, Boggs M, Beebe TP, Huang CP. Oxidation of single-walled carbon nanotubes in dilute aqueous solutions by ozone as affected by ultrasound. Carbon 2008;46(3):466–75.
[31] Simmons J, Nichols B, Baker S, Marcus MS, Castellini O, Lee C-S, Hamers R, Eriksson M. Effect of ozone oxidation on single-walled carbon nanotubes. J Phys Chem B 2006;110(14):7113–8.
[32] Chiang H-L, Chiang P, Huang C. Ozonation of activated carbon and its effects on the adsorption of VOCs exemplified by methylethylketone and benzene. Chemosphere 2002;47(3):267–75.
[33] Sham M-L, Kim J-K. Surface functionalities of multi-wall carbon nanotubes after UV/Ozone and TETA treatments. Carbon 2006;44(4):768–77.
[34] Tang L-c, Zhang H, Han J-h, Wu X-p, Zhang Z. Fracture mechanisms of epoxy filled with ozone functionalized multi-wall carbon nanotubes. Compos Sci Technol 2011;72(1):7–13.
[35] Najafi E, Kim J-Y, Han S-H, Shin K. UV-ozone treatment of multi-walled carbon nanotubes for enhanced organic solvent dispersion. Colloid Surf Physicochem Eng Asp 2006;284–285:373–8.
[36] Hydro RM, Pearson RA. Epoxies toughened with triblock copolymers. J Polym Sci B Polym Phys 2007;45(12):1470–81.

[37] Ruiz-Pérez L, Royston GJ, Fairclough JPA, Ryan AJ. Toughening by nanostructure. Polymer 2008;49(21):4475–88.
[38] Bahrami A, Cordenier F, Van Velthem P, Ballout W, Pardoen T, Nysten B, Bailly C. Synergistic local toughening of high performance epoxy-matrix composites using blended block copolymer-thermoplastic thin films. Compos Appl Sci Manuf 2016; 91:398–405.
[39] Chong H, Taylor A. The microstructure and fracture performance of styrene–butadiene–methylmethacrylate block copolymer-modified epoxy polymers. J Mater Sci 2013;48(19):6762–77.
[40] Gerard P, Boupat NP, Fine T, Gervat L, Pascault JP. Toughness properties of lightly crosslinked epoxies using block copolymers. Macromolecular Symposia. Wiley Online Library; 2007. p. 55–64.
[41] Chen J, Taylor AC. Epoxy modified with triblock copolymers: morphology, mechanical properties and fracture mechanisms. J Mater Sci 2012;47(11): 4546–60.
[42] Gómez-del Río T, Salazar A, Pearson R, Rodríguez J. Fracture behaviour of epoxy nanocomposites modified with triblock copolymers and carbon nanotubes. Compos B Eng 2016;87:343–9.
[43] Prolongo S, Gude M, Ureña A. Adhesive strength and toughness improvement of epoxy resin modified with polystyrene-b-polybutadiene-b-poly (methyl methacrylate) block copolymer. J Mater Sci Eng 2012;1(2). 2169-0022.1000109.
[44] Kahraman R, Sunar M, Yilbas B. Influence of adhesive thickness and filler content on the mechanical performance of aluminum single-lap joints bonded with aluminum powder filled epoxy adhesive. J Mater Process Technol 2008;205(1): 183–9.
[45] Liao L, Huang C, Sawa T. Effect of adhesive thickness, adhesive type and scarf angle on the mechanical properties of scarf adhesive joints. Int J Solids Struct 2013;50(25):4333–40.
[46] Rider A. Factors influencing the durability of epoxy adhesion to silane pretreated aluminium. Int J Adhesion Adhes 2006;26(1–2):67–78.
[47] Hong S-k, Kim D, Lee S, Kim B-W, Theilmann P, Park S-H. Enhanced thermal and mechanical properties of carbon nanotube composites through the use of functionalized CNT-reactive polymer linkages and three-roll milling. Compos Appl Sci Manuf 2015;77:142–6.
[48] Pal PP, Larionova T, Anoshkin IV, Jiang H, Nisula M, Goryunkov AA, Tolochko OV, Karppinen M, Kauppinen EI, Nasibulin AG. Dry functionalization and doping of single-walled carbon nanotubes by ozone. J Phys Chem C 2015;119(49):27821–8.
[49] Janarthanan V, Thyagarajan G. Miscibility studies in blends of poly (N-vinyl pyrrolidone) and poly (methyl methacrylate) with epoxy resin: a comparison. Polymer 1992;33(17):3593–7.
[50] Kwei T. The effect of hydrogen bonding on the glass transition temperatures of polymer mixtures. J Polym Sci, Polym Lett Ed 1984;22(6):307–13.
[51] Tseng C-H, Wang C-C, Chen C-Y. Functionalizing carbon nanotubes by plasma modification for the preparation of covalent-integrated epoxy composites. Chem Mater 2007;19(2):308–15.
[52] Allaoui A, El Bounia N-E. How carbon nanotubes affect the cure kinetics and glass transition temperature of their epoxy composites?–A review. 2009.
[53] Charles A, Rider A. Triblock copolymer toughening of a carbon fibre-reinforced epoxy composite for bonded repair. Polymers 2018;10(8):888.
[54] Gómez-del Río T, Rodríguez J, Pearson R. Compressive properties of nanoparticle modified epoxy resin at different strain rates. Compos B Eng 2014;57:173–9.
[55] Dean JM, Grubbs RB, Saad W, Cook RF, Bates FS. Mechanical properties of block copolymer vesicle and micelle modified epoxies. J Polym Sci B Polym Phys 2003; 41(20):2444–56.
[56] Liu J, Thompson ZJ, Sue H-J, Bates FS, Hillmyer MA, Dettloff M, Jacob G, Verghese N, Pham H. Toughening of epoxies with block copolymer micelles of wormlike morphology. Macromolecules 2010;43(17):7238–43.
[57] Abràmoff MD, Magalhães PJ, Ram SJ. Image processing with ImageJ. Biophot Int 2004;11(7):36–42.
[58] Rider A, Chalkley P. Durability of an off-optimum cured aluminium joint. Int J Adhesion Adhes 2004;24(2):95–106.